International Journal of Heat and Mass Transfer 54 (2011) 5298–5305

Contents lists available at SciVerse ScienceDirect

International Journal of Heat and Mass Transfer

journal homepage: www.elsevier.com/locate/ijhmt

Stability analysis and maldistribution control of two-phase flow in parallel evaporating channels

TieJun Zhang [a,b,*], John T. Wen [a,b,c], Agung Julius [c], Yoav Peles [b], Michael K. Jensen [b]

[a] Center for Automation Technologies and Systems, Rensselaer Polytechnic Institute, 110 8th Street, Troy, NY 12180, USA
[b] Department of Mechanical, Aerospace & Nuclear Engineering, Rensselaer Polytechnic Institute, 110 8th Street, Troy, NY 12180, USA
[c] Department of Electrical, Computer & System Engineering, Rensselaer Polytechnic Institute, 110 8th Street, Troy, NY 12180, USA

ARTICLE INFO

Article history:
Received 17 February 2011
Accepted 26 July 2011
Available online 29 August 2011

Keywords:
Flow instability
Flow distribution
Multiple evaporators
Parallel channel
Two-phase flow

ABSTRACT

Parallel channel heat transfer system is an attractive means to enhance heat transfer by increasing the total surface area in the heat exchanger. Uniform distribution of flow in the channels is an important operation attribute in order to avoid channel dryout and the subsequent hot spots and possible device failure. For the system operating in the single-phase regime, uniform flow distribution is a stable equilibrium. However, in the two-phase boiling regime, stable equilibrium bifurcates – the uniform distribution becomes unstable, and new stable or unstable non-uniform distributions, or maldistributions, equilibria emerge. As a result, parallel channel heat exchangers typically operate in the single phase regime to avoid such "maldistribution instability". This paper presents a stability analysis and active flow and temperature control of a parallel channel evaporator in a pumped two-phase boiling heat transfer loop. We show that for identical channels, the system is uncontrollable with the pump alone and unobservable from the overall flow rate measurement. A conventional solution involves introducing additional valve-induced pressure drop, but the drawback is a resulting higher pumping power. We present a new, somewhat surprising, result that if the channel characteristics are all distinct, the system actually becomes controllable from the pump and observable from the total loop flow rate. For non-identical parallel systems, we show a controller design approach and demonstrate its efficacy through a simulation example.

1. Introduction

Evaporating two-phase flow has been widely used in power generation, thermal management, chemical and other industries due to its excellent heat transfer performance [1–4]. For example, in next-generation solar thermal power plants, an array of parallel parabolic trough solar collectors are used to generate steam directly instead of using oil as the secondary heating medium [5,6]. The commercialization of large-scale direct steam generation technologies is hindered by the lack of understanding of two-phase flow behavior within the absorbing pipes and the fear of possible occurrence of critical heat flux, nonuniform heating, instabilities and uneven flow rate distribution [7,8]. Cooling is also a critical problem for high heat-flux electronics as heat is fast becoming the performance bottleneck [3,4,9]. Microchannel flow boiling is a promising approach as it utilizes both the latent heat of evaporation and the larger area to volume ratio in microchannels to enhance the heat transfer performance [1,10,11]. Much effort has been made to design boiling microchannel heat exchangers with a large number of parallel channels. Such a configuration is attractive as it maximizes the heat transfer with minimal pump demand [3,4,9,12].

Two-phase heat exchangers pose unique challenges as they are prone to various flow boiling instabilities [13], such as the Ledinegg flow excursion, parallel-channel flow maldistribution, pressure-drop and density-wave flow oscillations. The Ledinegg instability arises when the flow boiling system operates in the two-phase negative-slope region of the demand pressure curve, where the demand pressure drop decreases with increasing mass flow rate [12–15]. Slight changes in the supply pressure drop will trigger a sudden flow excursion to either a subcooled or a superheated operating condition. Pressure-drop oscillations could occur when there exists large upstream compressibility of the flow boiling system, pressure-drop oscillations [1,13]. For microchannel systems, flow has been observed to redistribute among the parallel channels in a nonuniform fashion both spatially and temporally. This "maldistribution instability" could cause large uncontrolled microchannel wall temperature difference. Different flow conditions were experimentally demonstrated and found to be heavily dependent on the prior state of the microchannels [16]. Even for conventional-scale two-phase heat exchangers, flow maldistribution also has dramatic negative

* Corresponding author at: Center for Automation Technologies and Systems, Rensselaer Polytechnic Institute, 110 8th Street, Troy, NY 12180, USA. Tel.: +1 518 276 2125; fax: +1 518 276 4897.
E-mail address: tjzhrpi@gmail.com (T.J. Zhang).

0017-9310/$ - see front matter © 2011 Elsevier Ltd. All rights reserved.
doi:10.1016/j.ijheatmasstransfer.2011.08.013

Nomenclature

A	cross-sectional area (m^2)	i	i-th channel
L	length (m)	in	inlet
N	channel number	e	exit
P	pressure (Pa)	w	wall
T	Temperature (°C)	r	restrictor
V	volume (m^3)	D	demand
ΔP	pressure drop (Pa)	S	supply
$\dot{m}$	mass flow rate (g/s)		
s	pressure drop slope (Pa s/g)	*Superscripts*	
t	time (s)	i	i-th channel
Subscripts			
0	initial		

consequences on thermal and mechanical performance [17,18]. Attributed to local flow instabilities and maldistribution, the critical heat flux condition could be prematurely initiated before the advantage of phase change is realized [19]. Local channel dryout would severely compromise heat transfer performance and could lead to severe safety problems.

In a parallel-channel flow boiling system, both pressure drop oscillations and non-uniform flow distributions take place under certain operating conditions. Experimental, analytical, and simulation studies have been reported to establish stability criteria [7,20–24] With the simplified parallel-pipe flow analysis by [25], a control procedure was proposed in [8] to regulate the individual pipe flow rates with a desired pipe exit quality through a set of inlet control valves. To suppress the two-phase flow instability in microchannels, the methods of inlet control valve [8], inlet restrictors [26] and inlet seed bubble generators [27] were proposed. Introducing these additional control devices leads to either larger pressure loss or higher power consumption, and increased fabrication costs. Active two-phase flow control offers the potential as an alternative to mitigate microchannel flow instabilities. In [28], we proposed a dynamic model-based pump control approach to suppress pressure-drop flow oscillations in microchannel boiling systems, where the inlet flow from the pump can be regulated to compensate for the upstream compressibility.

In this paper, we address the two-phase flow maldistribution instability among multiple parallel evaporating channels. Our focus is on using the pump to regulate the channel flow rather than regulating the pressure of the individual channels as in the past. A dual problem is to estimate the individual channel flow rates based on the measurement of the total flow rate. For heat exchangers with identical channels, the equilibria in the single-phase regimes (subcooled liquid or superheated vapor) for a given total flow rate are unique and globally stable. In the two-phase regime, the single-phase equilibria bifurcate to multiple equilibria, with the uniform flow equilibrium becoming unstable while the non-uniform flow equilibria are (locally) stable. Furthermore, the hope of using active feedback control to stabilize the unstable equilibrium is dashed as we show that the linearized system about the unstable equilibrium is neither controllable nor observable, implying that no linear time invariant stabilizing controller (or channel flow observer) exists. We are motivated by the observation that balancing multiple parallel inverted pendulums (i.e., multiple pendulums on a common cart) is controllable from the common base force *except* when the pendulums are identical. Similarly, the system is observable from the base motion except when the pendulums are identical. This also follows as a consequence of systems with symmetry requiring more than one control parameter [29]. Indeed, when the channels are non-identical, meaning that the slope of the pressure drop versus the mass flow curve at the unstable equilibrium is different for each channel, the system becomes both controllable from the pump and observable from the total mass flow rate. Once the controllability and observability properties are established, we develop a stabilizing feedback controller based on the model predictive control approach using the first-principle flow dynamics model. Simulation results have demonstrated that the open-loop unbalanced flow in parallel evaporating channels can be effectively regulated to the desired operating point with balanced two-phase flow distribution, resulting in improved two-phase heat transfer performance and lower channel surface temperatures.

2. Parallel channel flow stability

2.1. Stability analysis of parallel channels with inlet pressure control

Consider N parallel boiling channels with the same inlet and exit manifolds, as depicted in Fig. 1. The ith channel has length L and cross-sectional area A_i.

The overall mass flow rate through the boiling channels is $\dot{m} = \sum_{i=1}^{N} \dot{m}_i$, where $\dot{m}_i$ is the mass flow rate in the ith channel. Applying a momentum balance, we obtain [30]

$$\frac{L}{A_i}\frac{d\dot{m}_i}{dt} = \Delta P_S - \Delta P_D^i = P_{in} - P_e - \Delta P_D^i(\dot{m}_i), \tag{1}$$

where ΔP_s, the supply pressure drop is the difference between the inlet pressure, P_{in} (controlled by the pump), and the exit pressure, P_e, ΔP_D^i is the demand pressure drop of the i-th channel, with a typical shape as in Fig. 2. We assume that exit pressure P_e and temperature are maintained at a constant value by an external temperature controller immersed in the downstream reservoir.

If P_{in} is a constant, $P_{in} = P_{in}^*$, then the equilibria for channel i are given by the intersection between the horizontal line, $\Delta P_s^* = P_{in}^* - P_e$, and the demand pressure drop curve in Fig. 2:

$$\Delta P_s^* = P_{in}^* - P_e = \Delta P_D^i(\dot{m}_i^*). \tag{2}$$

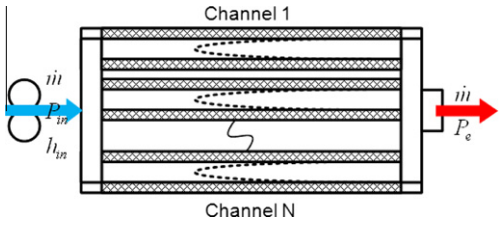

Fig. 1. Schematic of parallel boiling channels.

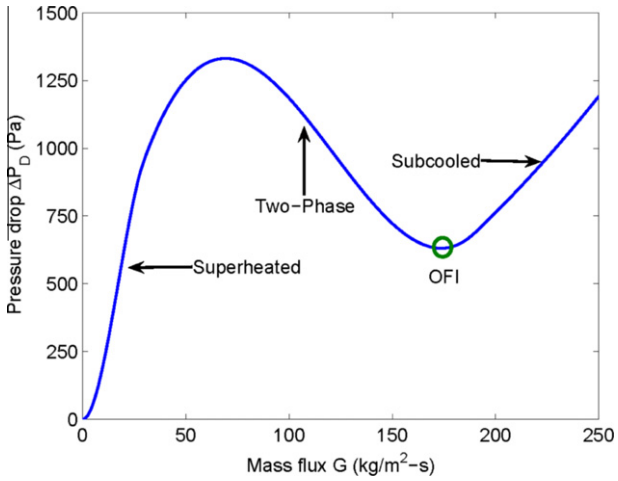

Fig. 2. Typical two-phase flow characteristics of a boiling channel under constant heat flux (OFI: onset of flow instability [15]; $G = \dot{m}/A$: mass flux).

For a given pressure drop, there may be up to three possible equilibria with flow rates corresponding to the subcooled, two-phase and superheated flows. For high and low pressure drops, there is only one equilibrium, corresponding to the subcooled and superheated flows, respectively.

With P_{in} as the control variable, we can analyze the stability of (1). For open loop system, i.e., P_{in} is a constant, the stability of the equilibria is determined by the linearized system

$$\frac{L}{A_i}\frac{d\delta\dot{m}_i}{dt} = -\frac{d\Delta P_D^i(\dot{m}_i^*)}{d\dot{m}_i}\delta\dot{m}_i. \tag{3}$$

Clearly, the equilibrium is stable if and only if the slope of the demand curve is positive. In the two-phase region, the slope of pressure-drop versus flow curve is negative, resulting in what is known as the Ledinegg Instability [13,15]. It should be noted that the pressure-drop slope depends on many flow system parameters (i.e., heat flux, inlet subcooling) as discussed in [15]; in this paper we focus on the mass flow effect.

A common solution to the two-phase instability problem is to add extra pressure drop through valving at each channel inlet. This increases the power requirement on the pump and adds implementation complexity. The problem is even more acute for microchannel evaporators where there may be more than 100 channels. If the pump alone is used to regulate the channel flows, then the linearized channel dynamics become coupled:

$$\frac{L}{A_i}\frac{d\delta\dot{m}_i}{dt} = \sum_{i=1}^{N}\frac{d(P_{in}(\dot{m}^*))}{d\dot{m}}\delta\dot{m}_i - \frac{d\Delta P_D^i(\dot{m}_i^*)}{d\dot{m}_i}\delta\dot{m}_i. \tag{4}$$

Writing the equation in the vector form, we have

$$\frac{d\delta\dot{m}_v}{dt} = \frac{\overline{A}\overline{D}^T\overline{D}s_{in}}{L}\delta\dot{m}_v - \frac{\overline{A}S}{L}\delta\dot{m}_v \tag{5}$$

where

$$\dot{m}_v = \begin{bmatrix}\dot{m}_1\\ \vdots \\ \dot{m}_N\end{bmatrix}, \quad \overline{D}^T = \begin{bmatrix}1\\ \vdots \\ 1\end{bmatrix}, \quad \overline{A} = \mathrm{diag}\{A_1,\ldots,A_N\},$$

$$s_{in} = \frac{d(P_{in}(\dot{m}^*))}{d\dot{m}}, \quad S = \mathrm{diag}\{s_1,\ldots,s_N\}, \quad s_i := \frac{d\Delta P_D^i(\dot{m}_i^*)}{d\dot{m}_i}. \tag{6}$$

As shown in Appendix A, the linearized system is stabilizable by choosing an appropriate s_{in} if and only if

$$\overline{D}^{\perp T}S\overline{D}^{\perp} > 0 \tag{7}$$

where >0 means that the matrix is positive definite, and $\overline{D}^{\perp} \in \mathbb{R}^{N\times N-1}$ is the orthogonal complement of $\overline{D}$, i.e., the rank $N-1$ matrix such that $\overline{D}\overline{D}^{\perp} = 0$. The matrix $\overline{D}^{\perp}$ is non-unique. In particular, we may choose it so that the columns are orthonormal, i.e.,

$$\overline{D}^{\perp T}\overline{D}^{\perp} = I_{N-1}. \tag{8}$$

For $N = 1$, $D^{\perp}$ is a null matrix, so (7) is satisfied. For $N = 2$, the condition becomes $s_1 + s_2 > 0$ (same as [20] where the condition was shown for $A_i = A$). For $N = 3$, using the principal minor test for positive definiteness, the condition becomes, $s_1 + s_2 > 0$ and $s_1s_2 + s_2s_3 + s_1s_3 > 0$. Conditions for other N's may be similarly calculated.

Note that a particular choice of s_{in} that will guarantee that the linearized system is stable under (7) is $s_{in} = -\infty$ (i.e., constant inlet flow rate). From (30) of Appendix A $a = -s_{in}N^2 + \overline{D}S\overline{D}^T$ will be $+\infty$, and $a - fS_1f^T$ is therefore always positive. Our stability criterion (7) is consistent with the criterion reported in [21], which is a special case of our result.

2.2. Stability analysis of parallel channels with upstream compressibility

To include the effect of flow compressibility, we include in the model an upstream surge tank [28], which is motivated by the compressible two-phase flow in a drum-boiler [2,31], as shown in Fig. 3. The governing equations become:

$$\frac{dP_{in}}{dt} = \frac{P_{in}^2}{\rho_l P_0 V_0}\left(\dot{m}_{in} - \sum_{i=1}^{N}\dot{m}_i\right) \tag{9}$$

$$\frac{d\dot{m}_i}{dt} = \frac{A_i}{L}\left(P_{in} - P_e - \Delta P_D^i(\dot{m}_i)\right) \tag{10}$$

where $\dot{m}_{in}$ is now the input variable (which is regulated by the pump). For a given $\dot{m}_{in}^*$, the equilibrium state $(P_{in}^*, \dot{m}_1^*, \ldots, \dot{m}_N^*)$ is given by

$$\sum_{i=1}^{N}\dot{m}_i^* = \dot{m}_{in}^* \tag{11}$$

$$\Delta P_D^i(\dot{m}_i^*) = \Delta P_D^j(\dot{m}_j^*), \quad \text{for all } i,j \in [1,N] \tag{12}$$

$$P_{in}^* = P_e + \Delta P_D^i(\dot{m}_i^*), \quad \text{for all } i \in [1,N]. \tag{13}$$

The equilibrium condition may be viewed in terms of the flow rate in each demand curve corresponding to the same channel pressure drop as illustrated in Fig. 4.

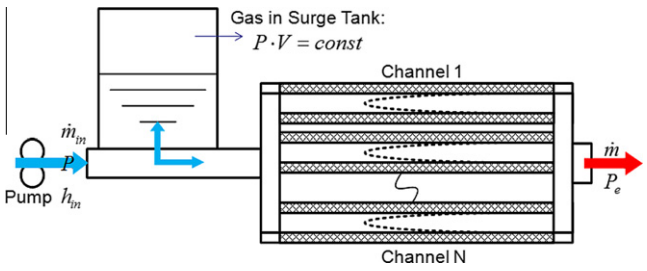

Fig. 3. Schematic of multiple parallel boiling channels with a upstream surge tank.

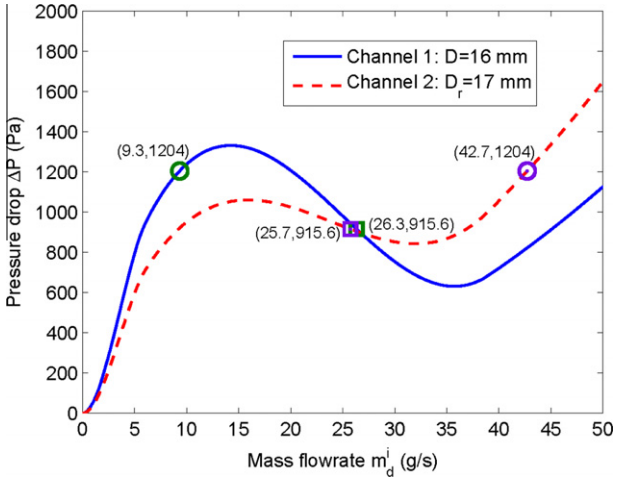

Fig. 4. Two-phase flow characteristics of two non-identical channels.

The linearized system about the equilibrium is

$$\begin{bmatrix} \frac{d\delta P_{in}}{dt} \\ \frac{d\delta \dot{m}_1}{dt} \\ \vdots \\ \frac{d\delta \dot{m}_N}{dt} \end{bmatrix} = \underbrace{\begin{bmatrix} 0 & -a & \cdots & -a \\ b_1 & -b_1 s_1 & \cdots & 0 \\ \vdots & & \ddots & 0 \\ b_N & 0 & \cdots & -b_N s_N \end{bmatrix}}_{\mathcal{A}} \begin{bmatrix} \delta P_{in} \\ \delta \dot{m}_1 \\ \delta \dot{m}_2 \\ \vdots \\ \delta \dot{m}_N \end{bmatrix} + \underbrace{\begin{bmatrix} a \\ 0 \\ \vdots \\ 0 \end{bmatrix}}_{\mathcal{B}} \delta \dot{m}_{in} \tag{14}$$

where

$$a = \frac{P_{in}^{*\,2}}{\rho_\ell P_0 V_0}, \quad b_i = \frac{A_i}{L}. \tag{15}$$

As shown in Appendix B, the condition for stability is the same as (7) with the additional condition

$$\overline{D}S\overline{D}^T = \sum_{i=1}^{N} s_i > 0. \tag{16}$$

This is because the upstream surge tank regulates P_{in} and plays a role similar to the direct manipulation of P_{in} as a function of $\dot{m}$ in (5), but this also incurs additional dynamics.

For identical channels, the balanced flow condition, $\dot{m}_i^* = \dot{m}^*/N$, is always at equilibrium, but it is unstable (s_i are all negative) in the two-phase regime, as shown in the bifurcation diagram Fig. 5 for the two-channel case. For non-identical channels, the bifurcation diagram as illustrated in Fig. 6 is more complex, but the balanced flow case in the two-phase regime is also unstable.

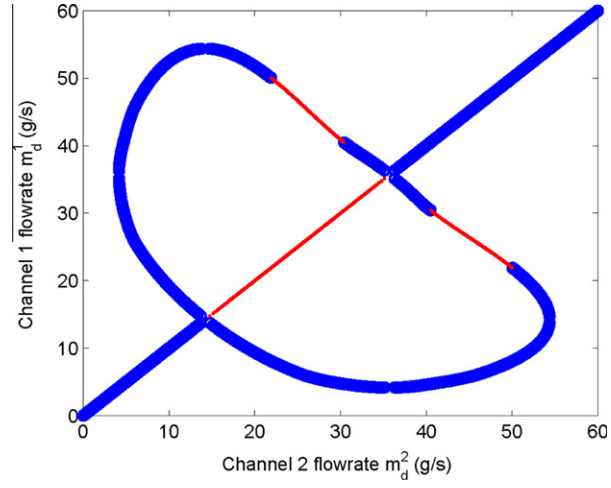

Fig. 5. Bifurcation curves of individual flow distribution $\dot{m}_1^*$ versus $\dot{m}_2^*$ in two identical parallel channels (blue: stable; red: unstable). (For interpretation of the references to colour in this figure legend, the reader is referred to the web version of this article.)

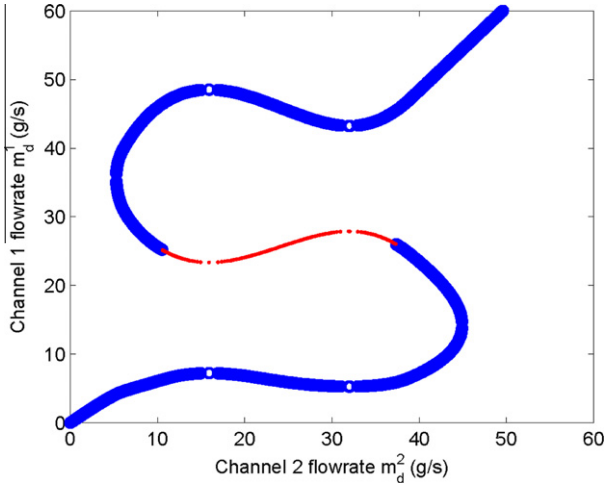

Fig. 6. Bifurcation curves of individual flow distribution $\dot{m}_1^*$ versus $\dot{m}_2^*$ in two non-identical parallel channels (blue: stable; red: unstable). (For interpretation of the references to colour in this figure legend, the reader is referred to the web version of this article.)

2.3. Controllability and observability

To explore the possibility of two-phase flow maldistribution control, the controllability and observability analysis [32] is essential. In the context of parallel-channel two-phase flow system in Fig. 3, the controllability means the possibility of using the pumped inlet total flow, $\dot{m}_{in}$, to regulate the individual channel flow, $\dot{m}_i$, to any desired state, i.e., a state such that the channel exit flow is of two phase (liquid vapor mixture) for better heat transfer performance; the observability means the possibility of using the total flow measurement, $\dot{m}$, to estimate the individual channel flow, $\dot{m}_i$.

The controllability for the linearized system (the ability of using the input to arbitrarily place the closed loop poles) corresponds to the full rank condition of the controllability matrix [32]:

$$\mathbb{C} = \begin{bmatrix} \mathcal{B} & \mathcal{A}\mathcal{B} & \cdots & \mathcal{A}^N\mathcal{B} \end{bmatrix} \tag{17}$$

With elementary row and column operations (which do not affect the rank), $\mathbb{C}$ becomes

$$\mathbb{C}_1 = \begin{bmatrix} 1 & 0 & 0 & \cdots & 0 \\ 0 & 1 & A_1 s_1 & \cdots & (A_1 s_1)^{N-1} \\ \vdots & \vdots & \vdots & \cdots & \vdots \\ 0 & 1 & A_N s_N & \cdots & (A_N s_N)^{N-1} \end{bmatrix}. \tag{18}$$

The lower portion of the matrix is a Vandermonde matrix [33]. Hence this matrix loses rank if and only if

$$A_i s_i = A_j s_j, \quad \text{for some } i \neq j. \tag{19}$$

or equivalently

$$\frac{d\Delta P_D^i(G_i^*)}{dG_i} = \frac{d\Delta P_D^j(G_j^*)}{dG_j}, \quad G_i = \frac{\dot{m}_i}{A_i}, \quad i \neq j. \tag{20}$$

This means if any of the two channels are identical in terms of channel geometry and pressure demand curve at the equilibrium, then the system is uncontrollable. For uniformly distributed flows in the two-phase regime, which we have seen to be unstable, the hope for feedback stabilization is lost if there is any channel symmetry.

The dual property of controllability is observability [32] –the ability to reconstruct the individual flow $\delta\dot{m}_i$ from the total flow $\delta\dot{m}$ based on the linearized model. Supposed that, $\dot{m} = \sum_{i=1}^{N}\dot{m}_i$, is the measured output:

$$\delta\dot{m} = \underbrace{\begin{bmatrix}0 & 1 & \cdots & 1\end{bmatrix}}_{\mathcal{C}} \begin{bmatrix}\delta P_{in}\\ \delta\dot{m}_1\\ \vdots\\ \delta\dot{m}_N\end{bmatrix}. \tag{21}$$

A necessary and sufficient condition for observability is the full-rankness of the observability matrix:

$$\mathbb{O} = \begin{bmatrix}\mathcal{C}\\ \mathcal{C}\mathcal{A}\\ \mathcal{C}\mathcal{A}^2\\ \vdots\\ \mathcal{C}\mathcal{A}^N\end{bmatrix}. \tag{22}$$

Using elementary row and column operations, $\mathbb{O}$ may be manipulated to

$$\mathbb{O}_1 = \begin{bmatrix} 0 & 1 & \cdots & 1\\ \sum_{i=1}^{N} b_i & b_1 s_1 & \cdots & b_N s_N\\ \sum_{i=1}^{N} b_i^2 s_i & (b_1 s_1)^2 & \cdots & (b_N s_N)^2\\ \vdots & \vdots & \vdots & \vdots\\ \sum_{i=1}^{N} b_i (b_i s_i)^{N-1} & (b_1 s_1)^N & \cdots & (b_N s_N)^N \end{bmatrix}. \tag{23}$$

We can further simplify this matrix as follows. Define a polynomial of degree N:

$$K(\lambda) \triangleq \prod_{i=1}^{N}(\lambda - s_i b_i) \triangleq \lambda^N + K_{N-1}\lambda^{N-1} + \cdots + K_0.$$

We then multiply the ith row by K_{i-1}, $i = 1,\ldots,N$, and add all of them to the last row. The resulting matrix is

$$\mathbb{O}_2 = \begin{bmatrix} 0 & 1 & \cdots & 1\\ \sum_{i=1}^{N} b_i & b_1 s_1 & \cdots & b_N s_N\\ \sum_{i=1}^{N} b_i^2 s_i & (b_1 s_1)^2 & \cdots & (b_N s_N)^2\\ \vdots & \vdots & \vdots & \vdots\\ -K_0 \sum_{i=1}^{N} \frac{1}{s_i} & 0 & \cdots & 0 \end{bmatrix}. \tag{24}$$

Note that $K_0 = \prod_i(-s_i b_i)$. As in the controllability case, this matrix consists of an $N \times N$ Vandermonde submatrix. The matrix loses rank if and only if $b_i s_i = b_j s_j$ (or, equivalently, $A_i\, s_i = A_j s_j$) for some $i \neq j$ or $K_0\sum_{i=1}^{N}\frac{1}{s_i} = 0$. If all channels operate in the same regime (liquid, two-phase, or vapor), then all s_i's are nonzero and have the same sign, and thus the additional condition is always satisfied.

When any two channels, i and j, are identical and the other channels are nonidentical, the reachable subspace, $\mathcal{R}$, is the span (all linear combinations) of $\delta P_{in}, \delta\dot{m}_i + \delta\dot{m}_j$, and all other $\delta\dot{m}_k, k \neq i,j$. The orthogonal complement of $\mathcal{R}, \mathcal{R}^{\perp}$, is the span of $\delta\dot{m}_i - \delta\dot{m}_j$. Similarly, we have the unobservable subspace $\mathcal{N} = \mathcal{R}^{\perp}$ and $\mathcal{N}^{\perp} = \mathcal{R}$. Representing the system using the decomposition of the state space, $\mathcal{R} \oplus \mathcal{R}^{\perp}$, partitions the system into a controllable and observable subsystem and an uncontrollable/unobservable subsystems. The uncontrollable/unobservable subsystem is unstable in the two-phase region (where the slope of the pressure demand curve is negative). Therefore, the system is unstabilizable and undetectable.

When two channels are almost identical, the system will be "close" to uncontrollability and unobservability, in the sense that the controllability matrix $\mathbb{C}$ and observability matrix $\mathbb{O}$ (or the controllability and observability grammians) are almost singular. This would result in large controller and observer gains which are highly undesirable due to input saturation and the lack of robustness to measurement delay and modeling error. The difference between the channels is characterized by the slopes of the channel demand pressure drop curve Eq. (20), which is a function of system pressure, mass flux, inlet subcooling, heat flux, hydraulic diameter, channel length, the type of working fluid, inlet restrictor [15] as well as channel surface roughness. They will need to be designed to achieve desired channel flow distribution and controllability/observability characteristics.

3. Flow stabilization in non-identical channels

When the flow operates in the two-phase regime, we have seen that the balanced flow equilibrium is unstable. Furthermore, if any two channels are identical, the linearized system about this equilibrium is neither controllable nor observable. In this section, we assume that the channel characteristics are all distinct, and we will design an active flow feedback controller to stabilize the unstable, but desirable, equilibrium.

The two-phase flow maldistribution has significant thermal consequences, which can be characterized by the wall energy balance equations. For individual evaporating channel, one has the evaporator wall temperature dynamics

$$\frac{dT_w^i}{dt} = \frac{q - q_r^i}{C_{pw}M_w}, \quad q_r^i = \alpha_r^i S_h\left(T_w^i - T_r^i\right), \tag{25}$$

where q is the imposed heat load, q_r^i is the actual heat transferred to the fluid (i.e., taking into account heat storage in wall), T_w^i is the ith evaporator wall temperature, T_r^i is the fluid saturation temperature, and the heat transfer coefficient α_r^i can be calculated based on Kandlikar's two-phase flow heat transfer and friction correlations [34]. When the heat load is very high, the channel exit flow becomes vapor only; hence, the local heat transfer performance deteriorate significantly, and the channel exit wall temperature becomes very high. In the thermal model (25) and subsequent study, only the exit wall temperature transient is indicated. For the simulation study, we consider the following evaporator parameters:

Channel length, L = 0.4 m
Cartridge heater diameter, D_c = 0.0127 m
Channel inner diameter, D_i = 0.0206 m
Hydraulic diameter, D = 0.0162 m
Cross-sectional area, $A = 2.0577 \times 10^{-4}$ m^2
Heated surface area, S_h = 0.0160 m^2
Wall thermal inertia, $C_{pw}M_w$ = 115.2 J/K

The working fluid is assumed to be the refrigerant R-134a. The cartridge heaters are used to represent the uniform heat load generated from electronics. These heaters, immersed in the refrigerant, emulate the evaporators in a two-phase cooling system. The operating conditions are selected below:

Imposed heat load, q = 1500 W
Inlet flow enthalpy, h_{in} = 55.1486 J/kg
Exit flow pressure, $P_e = 2 \times 10^5$ Pa
Initial system pressure, $P_0 = 2 \times 10^5$ Pa
Compressible gas volume, $V_0 = 0.7 \times 10^{-3}$ m^3

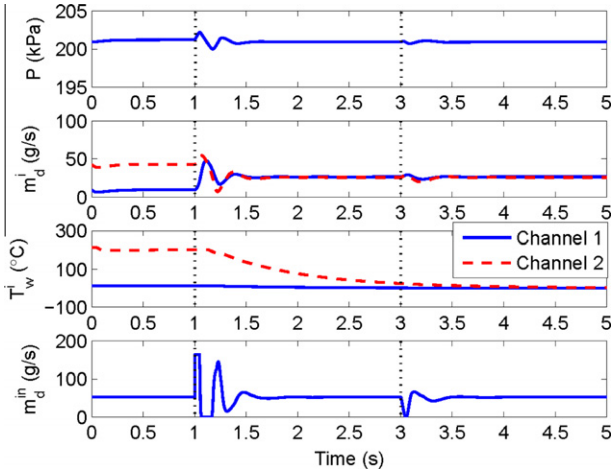

Fig. 7. Open-loop vs. closed-loop constrained linear quadratic regulator control responses: open-loop flow maldistribution [0–1] s, closed-loop balanced flow distribution [1–5] s, flow disturbance attenuation at $t = 3$ s (m_d^i: ith channel flow rate).

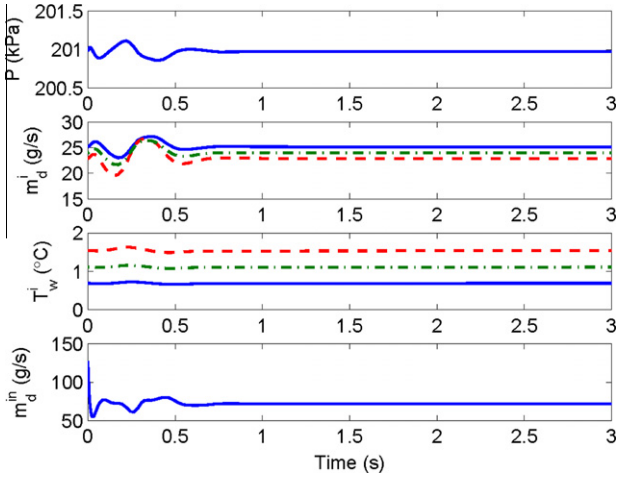

Fig. 9. Three-parallel-channel flow maldistribution control via linear quadratic regulator (m_d^i: individual channel flow rate; T_w^i: channel wall temperature).

Fig. 7 illustrates the active flow regulation about an unstable equilibrium in a two-channel system. In this study, a standard linear-quadratic-regulator (LQR) controller [32] is used, with a hard constraint imposed on the input flow control, $\dot{m}_{in} \in [0, 165]$ g/s. Model predictive control (MPC) may be applied to more effectively deal with the control constraints by solving a constrained optimization problem while maintaining the closed-loop system stability [35], but will not be pursued in this paper.

For two non-identical parallel channels, open-loop and closed-loop simulation results are shown in Fig. 7. The simulation is divided into three time zones:

- Open loop for $t < 1$ s: With $\dot{m}_{in} = 52$ g/s and no feedback control before $t = 1$ s, two-phase flow maldistribution occurs (corresponding to the circles in Fig. 4). In particular, channel 2 is subcooled with high mass flow rate, resulting in a very high wall temperature for that channel. At this initial maldistribution equilibrium, $P = 201.2$ kPa, $\dot{m}_1 = 9.3$ g/s, $\dot{m}_2 = 42.7$ g/s, $T_1 = 0.9\,^{\circ}$C, $T_2 = 201.1\,^{\circ}$C.
- LQR Control for $t \geqslant 1$ s: The active feedback control (using the full state feedback in this case) stabilizes the flow about the desired balanced flow equilibrium (corresponding to the squares in Fig. 4). The high wall temperature of channel 2 is now reduced to the level of channel 1 due to the improved heat transfer performance.
- Pulse exit flow disturbance at $t \in [3, 3.05]$ s: Even in the presence of a pulsed disturbance, the balanced flow distribution is still maintained.

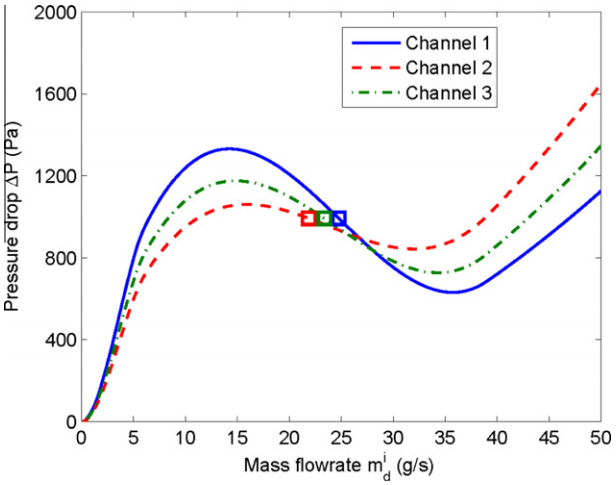

Fig. 8. Two-phase flow characteristics of three non-identical channels.

At the stabilized and balanced flow equilibrium, $P = 200.9$ kPa, $\dot{m}_1 = 26.3$ g/s, $\dot{m}_2 = 25.7$ g/s, $T_1 = 0.6$°C, $T_2 = 3.2$°C, and the eigenvalues of $\mathcal{A}$ for the open-loop unstable flow system (14) are $7.2504 + 12.2950i$, $7.2504 - 12.2950i$, 21.4465. The singular values of the controllability matrix (17) are 11748, 239, 3, and the singular value of the observability matrix (22) are 6411, 231, 7, evidently, both of them are of full rank.

In this simulation study, the weight matrices of the LQR cost function are chosen as $Q = 0.001 \cdot I_3$, $R = 0.1$, and the optimal gain matrix K is obtained as $K = [-1.6383, 10.8404, -46.9680]$.

We have also considered a three-channel example. The demand curves are shown in Fig. 8. At $t = 0$, a pulse input flow disturbance is applied. The LQR controller is able to maintain the equilibrium after a short transient, as shown in Fig. 9.

4. Conclusions

This paper analyzes the stability, controllability, and observability of parallel-channel two-phase flow systems. Although an inlet control valve for each individual channel can achieve a uniform two-phase flow distribution, the drawback is that the flow system has to sustain a higher pressure loss and the instrumentation is more complex. When the upstream pump is used as the control variable for an identical-channel flow system, it is only possible for the control of pressure-drop flow oscillations but not for the control of flow in the individual channels at the desired balanced flow equilibrium, which is open loop unstable. We demonstrate that a necessary and sufficient condition for the balanced flow equilibrium to be controllable is that the flow characteristics of each channel must be distinct. Similarly, as a dual result, the channel flow rates are not observable from the total flow rate under the identical-channel (between any two channels) case, but are observable when the channels characteristics are all distinct. Most microchannel heat sinks are fabricated to have multiple uniform parallel channels. This paper shows that from the control point of view, this is actually undesirable. We are now actively pursuing this research direction to exploit non-identical channel designs.

Acknowledgments

This work is supported in part by the Office of Naval Research (ONR) under the Multidisciplinary University Research Initiative (MURI) Award N00014-07-1-0723 entitled "System-Level Approach for Multi-Phase, Nanotechnology Enhanced Cooling of High-Power Microelectronic Systems," and in part by the Center for Automation Technologies and Systems (CATS) under a block grant from the New York State Foundation for Science, Technology and Innovation (NYSTAR). The first author would also like to acknowledge the partial support from the City University of Hong Kong (SRG7008093) for this work.

Appendix A. Open loop stability condition with inlet pressure control

We can write the system matrix in (5) as

$$\overline{A}_c = \frac{\overline{A}}{L}(\overline{D}^T\overline{D}s_{in} - S). \tag{26}$$

Applying similarity transform by pre- and post-multiplying $\overline{A}_c$ by $\overline{A}^{\frac{1}{2}}$ and $\overline{A}^{-\frac{1}{2}}$, respectively, we get

$$L\overline{A}^{\frac{1}{2}}\overline{A}_c\overline{A}^{-\frac{1}{2}} = \overline{A}^{\frac{1}{2}}(\overline{D}^T\overline{D}s_{in} - S)\overline{A}^{\frac{1}{2}}$$

which is a symmetric matrix. The stability of the system is then equivalent to $\overline{A}^{\frac{1}{2}}(\overline{D}^T\overline{D}s_{in} - S)\overline{A}^{\frac{1}{2}} < 0$. Since $\overline{A}^{\frac{1}{2}}$ is symmetric (in fact, diagonal) and invertible, this condition is further equivalent to

$$\overline{D}^T\overline{D}s_{in} - S < 0. \tag{27}$$

Let $\overline{D}^{\perp} \in \mathbb{R}^{N\times N-1}$ be the orthogonal complement of $\overline{D}^T$, i.e.,

$$\overline{D}\overline{D}^{\perp} = 0$$
$$\overline{D}^{\perp T}\overline{D}^{\perp} > 0.$$

The $N \times N$ matrix $\begin{bmatrix}\overline{D}^T & \overline{D}^{\perp}\end{bmatrix}$ is therefore invertible and (27) is equivalent to

$$\begin{bmatrix}\overline{D} \\ \overline{D}^{\perp T}\end{bmatrix}(-\overline{D}^T\overline{D}s_{in} + S)\begin{bmatrix}\overline{D}^T & \overline{D}^{\perp}\end{bmatrix} > 0. \tag{28}$$

This may be further manipulated to

$$M = \begin{bmatrix} a & f \\ f^T & S_1\end{bmatrix} > 0 \tag{29}$$

where

$$a = -s_{in}N^2 + \overline{D}S\overline{D}^T, \quad f = \overline{D}S\overline{D}^{\perp}, \quad S_1 = \overline{D}^{\perp T}S\overline{D}^{\perp}.$$

Since s_{in} is assumed to be arbitrary, a can be made an arbitrary positive number. Using the principal minor criterion for positive definiteness, the matrix M is positive definite if and only if $S_1 > 0$ and $\det M > 0$. The determinant of M may be expressed as

$$\det(M) = \det(S_1)(a - fS_1f^T). \tag{30}$$

Since a may be made arbitrarily large, we have $M > 0$ if and only if $S_1 > 0$, or

$$\overline{D}^{\perp T}S\overline{D}^{\perp} > 0. \tag{31}$$

Appendix B. Open loop stability condition with upstream surge tank

In this section, we will show that the system matrix, $\mathcal{A}$, of the linearized system (14) is identical to the stability condition (7) of the parallel-channel system with direct inlet pressure regulation.

Write $\mathcal{A}$ as

$$\mathcal{A} = \begin{bmatrix} 0 & -a\overline{D} \\ \frac{\overline{A}\overline{D}^T}{L} & -\frac{\overline{A}S}{L}\end{bmatrix} \tag{32}$$

with $\overline{D}, \overline{A}, S$ and a defined as in (6) and (15). An eigenvalue λ of $\mathcal{A}$ satisfies

$$\begin{bmatrix} 0 & -a\overline{D} \\ \frac{\overline{A}\overline{D}^T}{L} & -\frac{\overline{A}S}{L}\end{bmatrix}\begin{bmatrix} z \\ x\end{bmatrix} = \lambda\begin{bmatrix} z \\ x\end{bmatrix} \tag{33}$$

where $\begin{bmatrix} z & x^T\end{bmatrix}^T$ is the corresponding eigenvector. Expanding the equation, we have

$$-a\overline{D}x = \lambda z \tag{34}$$
$$\overline{A}\overline{D}^T z - \overline{A}Sx = \lambda Lx. \tag{35}$$

Since $\overline{A}$ is invertible, and $\overline{D}^{\perp T}\overline{D}^T = 0$, we have from (35):

$$-\overline{D}^{\perp T}Sx = \lambda L\overline{D}^{\perp T}\overline{A}^{-1}x. \tag{36}$$

If we set $x = \overline{D}^{\perp}y$, then we have a generalized eigenvalue problem

$$-\overline{D}^{\perp T}S\overline{D}^{\perp}y = \lambda L\overline{D}^{\perp T}\overline{A}^{-1}\overline{D}^{\perp}y. \tag{37}$$

Since $\overline{D}^{\perp T}\overline{A}^{-1}\overline{D}^{\perp}$ is positive definite, all N eigenvalues are negative if and only if

$$\overline{D}^{\perp T}S\overline{D}^{\perp} > 0$$

which is the same as (7).

There is one additional eigenvalue (from the compressibility of the flow). We now multiply (35) by $\overline{D}$ to obtain

$$\overline{D}\overline{D}^T z - \overline{D}Sx = \lambda L\overline{D}\overline{A}^{-1}x.$$

Note that $\overline{D}\overline{D}^T = \overline{N}$. Solve for z and substitute into (34), we have

$$\lambda(\overline{D}S + \lambda L\overline{D}\overline{A}^{-1})x = -a\overline{N}\overline{D}x.$$

Choose $x = \overline{D}^T$, we obtain a quadratic equation of λ:

$$L\overline{D}\overline{A}^{-1}\overline{D}^T\lambda^2 + \overline{D}S\overline{D}^T\lambda + a\overline{N}^2 = 0. \tag{38}$$

The roots will be negative if and only if

$$\overline{D}S\overline{D}^T = \sum_{i=1}^{N} s_i > 0.$$

References

[1] A.E. Bergles, J.H. Lienhard, et al., Boiling and evaporation in small diameter channels, Heat Transf. Eng. 24 (2003) 18–40.
[2] K.J. Astrom, R.D. Bell, Drum-boiler dynamics, Automatica 36 (2000) 363–378.
[3] S.V. Garimella, A.S. Fleischer, J.Y. Murthy, et al., Thermal challenges in next-generation electronic systems, IEEE Trans Compo. Packaging Tech. 31 (2008) 801–815.
[4] S.G. Kandlikar, A.V. Bapat, Evaluation of jet impingement, spray and microchannel chip cooling options for high heat flux removal, Heat Transfer Eng. 28 (2007) 911–923.
[5] L. Valenzuela, E. Zarza, et al., Direct steam generation in solar boilers, IEEE Contr. Syst. Mag. 24 (2004) 15–29.
[6] M. Eck, T. Hirsch, Dynamics and control of parabolic trough collector loops with direct steam generation, Sol. Energy 81 (2007) 268–279.
[7] S. Natan, D. Barnea, Y. Taitel, Direct steam generation in parallel pipes, Int. J. Multiphase Flow 29 (2003) 1669–1683.
[8] Y. Taitel, U. Minzer, D. Barnea, A control procedure for the elimination of mal flow rate distribution in evaporating flow in parallel pipes, Sol. Energy 82 (2008) 329–335.
[9] J. Lee, I. Mudawar, Low-temperature two-phase microchannel cooling for high-heat-flux thermal management of defense electronics, IEEE Trans. Compo Packaging Tech. 32 (2009) 453–465.
[10] S.G. Kandlikar, S. Garimella, et al., Heat Transfer and Fluid Flow in Minichannels and Microchannels, Elsevier, 2006.
[11] J.R. Thome, State-of-the-art overview of boiling and two-phase flows in microchannels, Heat Transf. Eng. 27 (2006) 4–19.

[12] J. Xu, J. Zhou, Y. Gan, Static and dynamic flow instability of a parallel microchannel heat sink at high heat fluxes, Energ. Convers. Manag. 46 (2005) 313–334.
[13] S. Kakac, B. Bon, A review of two-phase flow dynamic instabilities in tube boiling system, Int. J Heat Mass Transfer 51 (2008) 399–433.
[14] J. Yin, Modeling and analysis of multiphase flow instabilities, Ph.D thesis, Rensselaer Polytechnic Institute, 2004.
[15] T.J. Zhang, T. Tong, Y. Peles, et al., Ledinegg instability in microchannels, Int. J. Heat Mass Transfer 52 (2009) 5661–5674.
[16] R.D. Flynn, D.W. Fogg, et al., Boiling flow interaction between two parallel channels, in: Proceedings of 2006 ASME International Mechanical Engineering Congress & Exposition, Chicago, IL, 2006.
[17] J.B. Kitto, J.M. Robertson, Effects of maldistribution of flow on heat transfer equipment performance, Heat Transfer Eng. 10 (1) (1989) 18–25.
[18] A.C. Mueller, J.P. Chiou, Review of various types of flow maldistribution in heat exchangers, Heat Transfer Eng. 9 (2) (1988) 36–50.
[19] A.E. Bergles, S.G. Kandlikar, On the nature of critical heat flux in microchannels, ASME J. Heat Transf. 127 (1) (2005) 101–107.
[20] M. Ozawa, K. Akagawa, T. Sakaguchi, Flow instabilities in parallel-channel flow systems of gas–liquid two-phase flow mixtures, Int. J. Multiphase Flow 15 (1989) 639–657.
[21] K. Akagawa, T. Sakaguchi, M. Kono, M. Nishimura, Study on distribution of flow rates and stabilities in parallel long evaporators, Bull. JSME 14 (1971) 837–848.
[22] U. Minzer, D. Barnea, Y. Taitel, Evaporation in parallel pipes-splitting characteristics, Int. J. Multiphase Flow 30 (2004) 763–777.
[23] L. Pustylnik, D. Barnea, Y. Taitel, Prediction of two-phase flow distribution in parallel pipes using stability analysis, AICHE J. 52 (2006) 3345–3352.
[24] A. Kosar, C.-J. Kuo, Y. Peles, Suppression of boiling flow oscillations in parallel microchannels with inlet restrictors, J. Heat Transf. 128 (3) (2006) 251–260.
[25] U. Minzer, D. Barnea, Y. Taitel, Flow rate distribution in evaporating parallel pipes – modeling and experimental, Chem. Eng. Sci. 61 (2006) 7249–7259.
[26] C.-J. Kuo, Y. Peles, Pressure effects on flow boiling instabilities in parallel microchannels, Int. J. Heat Mass Transfer 52 (2009) 271–280.
[27] J. Xu, G. Liu, et al., Seed bubbles stabilize flow and heat transfer in parallel microchannels, Int. J. Multiphase Flow 35 (2009) 773–790.
[28] T.J. Zhang, Y. Peles, J.T. Wen, et al., Analysis and active control of pressure-drop flow instabilities in boiling microchannel systems, Int. J. Heat Mass Transf. 53 (2010) 2347–2360.
[29] R.O. Grigoriev, Symmetry and control: spatially extended chaotic systems, Physica D 140 (2000) 171–193.
[30] T.J. Zhang, J.T. Wen, Y. Peles, et al., Two-phase refrigerant flow instability analysis and active control in transient electronics cooling systems, Int. J. Multiphase Flow 37 (1) (2011) 84–97.
[31] J. Eborn, On model libraries for thermo-hydraulic applications, Ph.D thesis, Department of Automatic Control, Lund Institute of Technology, Sweden, 2001.
[32] K. Ogata, Modern Control Engineering, 5th ed., Prentice Hall, Upper Saddle River, N.J., 2008.
[33] G.H. Golub, C.F. Van Loan, Matrix Computations, 3rd ed., Johns Hopkins University Press, 1996.
[34] S.G. Kandlikar, A general correlation for two-phase flow boiling heat transfer inside horizontal and vertical tubes, ASME J. Heat Transf. 112 (1990) 219–228.
[35] D.Q. Mayne, J.B. Rawings, C.V. Rao, Constrained model predictive control: stability and optimality, Automatica 36 (2000) 789–814.